Доклади на Българската академия на науките
Comptes rendus de l'Académie bulgare des Sciences

Tome 78, No 10, 2025

ENGINEERING SCIENCES

Automatics and informatics

COMPACT DUAL-BAND HIGH-GAIN MIMO ANTENNA WITH MULTI-STAGE NOTCHED MICROSTRIP DESIGN FOR SUB-THZ COMMUNICATIONS

Abdelbasset Azzouz[1], Rachid Bouhmidi[1], Mohammed Chetioui[1], Zahriladha Zakaria[2], Ahmed Jamal Abdullah Al-Gburi[2]✉

Received on June 17, 2025
Presented by Ch. Roumenin, Member of BAS, on June 28, 2025

Abstract

This paper presents a compact two-port MIMO antenna designed for 0.1–1 THz applications. The antenna features a multi-stage notched microstrip patch, fed by a 50-ohm line with a 0.02 mm feed width, built on a polyimide substrate (thickness: 0.04 mm, $\varepsilon_r = 4.3$, loss tangent = 0.004). With a footprint of $0.4 \times 0.79\,\text{mm}^2$, it resonates at 0.372 THz and 0.762 THz, offering bandwidths of 20 GHz and 60 GHz.

Simulations using HFSS v15 show return losses of −30.73 dB and −31.76 dB, VSWRs of 1.06 and 1.05, and high gains of 5.00 dBi and 13.30 dBi. The design ensures strong isolation (ECC < 0.02), making it suitable for compact, high-gain THz MIMO systems.

Key words: compact design, dual-band, ECC, HFSS, high gain, terahertz antenna

1. Introduction. The rapid evolution toward sixth-generation (6G) wireless systems is driving the exploration of the terahertz (THz) band (0.1–10 THz), promising ultra-high data rates, sub-millisecond latency, and compact integration with intelligent nanoscale devices [1, 2].

The authors would like to thank Universiti Teknikal Malaysia Melaka (UTeM) and the Ministry of Higher Education (MOHE) of Malaysia for supporting this project.

https://doi.org/10.7546/CRABS.2025.10.08

However, designing efficient, high-gain, and miniaturized antennas that operate across wide bandwidths in the THz spectrum remains a formidable challenge due to high propagation losses, mutual coupling, and fabrication constraints at microscale dimensions [3, 4].

Recent advancements have offered promising directions. The integration of metamaterial structures has led to significant improvements in antenna gain and directivity. For instance, Benkhallouk et al. [5] employed dielectric superstrates and D-SRR configurations to enhance gain and directivity for imaging applications. Similarly, Ahammed et al. [6] and Amraoui et al. [7] designed MIMO systems with metamaterial loading and defected ground structures (DGS), achieving high isolation and gain. Amraoui et al. further explored frequency-selective surfaces (FSSs) [8] and linear MIMO arrays [9] for compact multi-port architectures with reduced envelope correlation coefficients (ECC).

Moreover, the works of Alibakhshikenari et al. [3] and Raghunath et al. [4] demonstrated on-chip and compact quad-port THz antennas capable of operating within 0.2–13 THz, targeting high-speed, high-isolation use cases. From a systems perspective, recent reviews by Ning et al. [1], Bodet et al. [2], and Diez-Comas et al. [10] have highlighted the role of spatial beamforming, leaky-wave arrays, and directional antennas in enabling high-capacity sub-THz MIMO communication.

Despite these advancements, a gap persists: most reported designs optimize gain, bandwidth, or isolation independently but fall short of providing a holistic solution that offers high directional gain, wide dual-band coverage, ultra-compactness, and robust MIMO performance within the lower sub-THz spectrum (0.1–1 THz). This frequency range is especially relevant for integrated THz transceivers in 6G-enabled IoT, nano-communication, and medical sensing applications where space, efficiency, and spectral agility are paramount.

To address this, we propose a compact two-port THz MIMO antenna optimized for the 0.1–1 THz range, leveraging a multi-stage notched microstrip patch on a polyimide substrate ($\varepsilon_r = 4.3$, $\tan\delta = 0.004$). With a footprint of only $0.4 \times 0.79\,\mathrm{mm}^2$, the antenna achieves dual resonances at 0.372 THz and 0.762 THz, supporting wide bandwidths of 20 GHz and 60 GHz, respectively. Simulations in Ansys HFSS v15 show excellent impedance matching ($S_{11} < -30\,\mathrm{dB}$), high gains (5.00 and 13.30 dBi), and low ECC (< 0.02), confirming the design's suitability for compact, high-throughput 6G applications. Unlike previous works, our antenna delivers high gain, wideband dual-band operation, strong MIMO isolation, and low-profile geometry in one unified structure, filling a critical gap in the state-of-the-art.

The remainder of this paper is organized as follows. Section 2 details the antenna design methodology and simulation setup. Section 3 presents and analyzes the simulation results, including return loss, VSWR, gain, and radiation patterns. Finally, Section 4 concludes the paper.

2. Antenna design. The proposed two-port MIMO antenna is developed for terahertz (THz) communication systems spanning the 0.1–1 THz frequency range. It employs a notched microstrip patch architecture that enables dual-resonant behaviour while maintaining compactness and isolation. The structure is built on a polyimide substrate with a thickness of 0.04 mm, relative permittivity $\varepsilon_r = 4.3$, and loss tangent of 0.004. The bottom surface of the polyimide substrate is fully metallized with copper to form the ground plane. A 50-ohm microstrip line with a feed width of 0.02 mm is used to excite each radiating element.

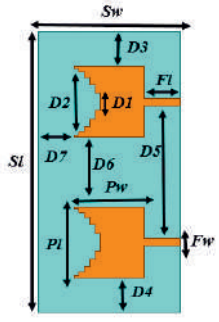

(a) Front view of the proposed antenna

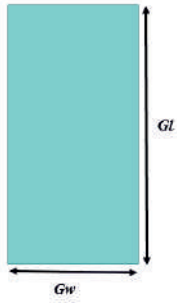

(b) Back view of the proposed antenna

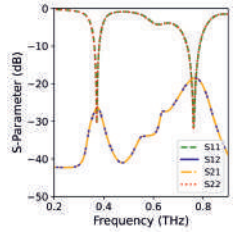

(c) Scattering parameters vs frequency

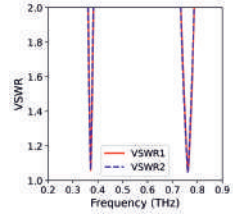

(d) VSWR of the proposed antenna

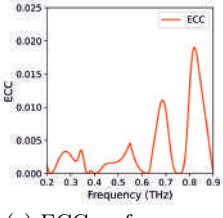

(e) ECC vs frequency

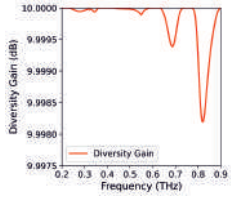

(f) Diversity Gain vs frequency

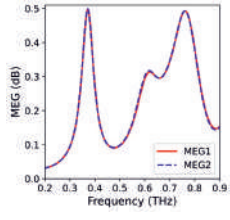

(g) Mean Effective Gain vs frequency

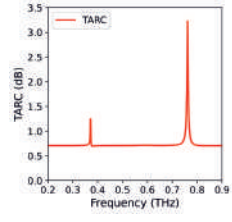

(h) Total Active Reflection Coefficient vs frequency

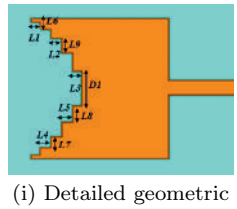

(i) Detailed geometric dimensions of the multi-stage notch

Fig. 1. Simulated antenna design and performance: (a) Front and (b) Back views, (c) Scattering parameters, (d) VSWR, (e) ECC, (f) Diversity Gain, (g) Mean Effective Gain, (h) Total Active Reflection Coefficient, (i) Detailed geometric dimensions of the multi-stage notch

The antenna occupies an ultra-compact footprint of $0.4 \times 0.79\,\mathrm{mm}^2$, making it suitable for integration in next-generation THz modules. Figure 1(a), (b), and (i) illustrates the front, back views and the detailed geometric dimensions of the multi-stage notch of the proposed antenna, respectively, while the corresponding design parameters are summarized in Table 1.

Table 1

Geometrical dimensions of the proposed antenna

Parameter	**Value (mm)**	**Parameter**	**Value (mm)**
S_w	0.40	G_l	0.79
S_l	0.79	F_w	0.02
P_l	0.20	F_l	0.10
P_w	0.20	D_1	0.05
G_w	0.40	D_2	0.19
L_1	0.015	L_2	0.015
L_3	0.015	L_4	0.015
L_5	0.015	L_6	0.01
L_7	0.015	L_8	0.025
D_3	0.1	D_4	0.1
D_5	0.38	D_6	0.2
D_7	0.108	L_9	0.02

The patch geometry is modelled using standard design principles of rectangular microstrip antennas. The resonant frequency of the dominant TM_{10} mode can be approximated as

$$f_r = \frac{c}{2L\sqrt{\varepsilon_{\text{eff}}}}, \tag{1}$$

where c is the speed of light, L is the effective patch length, and ε_{eff} is the effective dielectric constant, given by

$$\varepsilon_{\text{eff}} = \frac{\varepsilon_r + 1}{2} + \frac{\varepsilon_r - 1}{2}\left(1 + 12\frac{h}{W}\right)^{-1/2}. \tag{2}$$

The effective length L_{eff} accounts for fringe effects and is expressed as

$$L_{\text{eff}} = L + 2\Delta L \tag{3}$$

with the edge extension ΔL calculated by

$$\Delta L = 0.412h \cdot \frac{(\varepsilon_{\text{eff}} + 0.3)\left(\frac{W}{h} + 0.264\right)}{(\varepsilon_{\text{eff}} - 0.258)\left(\frac{W}{h} + 0.8\right)}. \tag{4}$$

These equations guide the preliminary dimensioning before optimization via full-wave simulations using Ansys HFSS.

3. Results and discussion. The simulated results validate the superior performance of the proposed compact THz MIMO antenna across multiple key metrics. As depicted in Fig. 1(e), the Envelope Correlation Coefficient (ECC) remains consistently below 0.02 throughout the operational band, indicating excellent isolation between ports and minimal correlation, which is vital for spatial diversity. This translates into a near-ideal Diversity Gain (DG) of 10 dB, as illustrated in Fig. 1(f), ensuring robust MIMO performance under multipath conditions.

The Mean Effective Gain (MEG) values for both ports lie within the optimal range of 0 to 0.5 (Fig. 1(g)), reflecting balanced reception power and confirming the antenna's efficiency in multipath-rich environments. The Total Active Reflection Coefficient (TARC), presented in Fig. 1(h), varies between 0.5 and 3.5, indicating acceptable active matching characteristics under simultaneous excitation.

In terms of impedance matching, the proposed antenna exhibits two well-defined resonances at 0.372 THz and 0.762 THz, with return losses of −30.73 dB and −31.76 dB, respectively, (Fig. 1(c)), and corresponding VSWR values of 1.06 and 1.05 (Fig. 1(d)). These values confirm excellent matching performance across a wide operational bandwidth of 20–60 GHz.

As shown in Fig. 2(a) and (b), the antenna achieves high realized gain levels

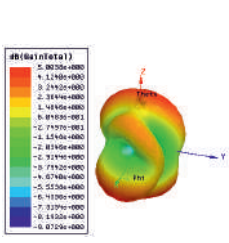

(a) Gain at 0.372 THz

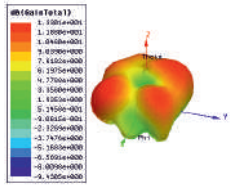

(b) Gain at 0.762 THz

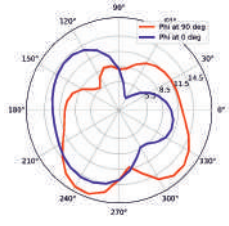

(c) Radiation pattern at 0.372 THz

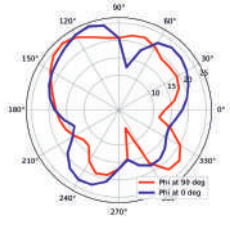

(d) Radiation pattern at 0.762 THz

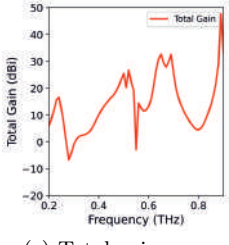

(e) Total gain over frequency

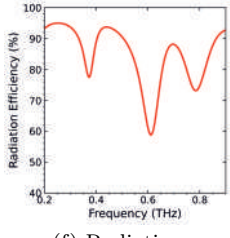

(f) Radiation Efficiency over frequency

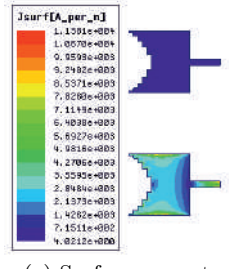

(g) Surface current distribution at 0.372 THz

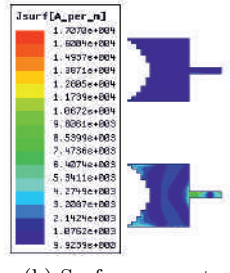

(h) Surface current distribution at 0.762 THz

Fig. 2. Simulated gain, radiation patterns, and performance metrics of the proposed antenna: (a) Gain at 0.372 THz, (b) Gain at 0.762 THz, (c) Radiation pattern at 0.372 THz, (d) Radiation pattern at 0.762 THz, (e) Total gain over frequency, (f) Radiation Efficiency over frequency, (g) Surface current distribution at 0.372 THz, (h) Surface current distribution at 0.762 THz

of 5.00 dBi and 13.30 dBi at the two resonant frequencies, respectively. Furthermore, the gain profile across the entire frequency range (Fig. 2(e)) remains stable, while the radiation efficiency exceeds 94% (Fig. 2(f)), further emphasizing the suitability of the design for high-speed THz wireless communication systems. The radiation patterns and current distribution (Fig. 2(c, d, g, h)) confirm the antenna's directional characteristics and efficient radiation at both resonant modes.

As shown in Fig. 2(c) and (d), the radiation patterns at 0.372 THz and 0.762 THz exhibit different main beam directions. This shift in the maximum radiation direction is primarily due to the change in operating frequency, which alters the effective electrical length of the slot and the phase distribution across the aperture. At higher frequencies, the wavelength becomes shorter, which can cause the radiation to become more directional or steer in a different angle. Additionally, the dimensions of the multi-stage slots significantly influence both impedance matching and radiation characteristics. By varying the slot lengths, widths, and spacing, the structure supports multiple resonances and controls current distribution along the surface, enabling better matching and shaping of the radiation pattern. These design choices directly affect how energy is radiated at each frequency, leading to the observed directional differences.

For a two-port MIMO antenna system, the ECC can be approximated using S-parameters as

$$\text{ECC} \approx \frac{|S_{11}^* S_{12} + S_{21}^* S_{22}|^2}{(1 - |S_{11}|^2 - |S_{21}|^2)(1 - |S_{22}|^2 - |S_{12}|^2)}. \tag{5}$$

Diversity Gain is derived from ECC as

$$\text{DG} = 10\sqrt{1 - (\text{ECC})^2}. \tag{6}$$

The Mean Effective Gain (MEG) for each port is calculated by

$$\text{MEG}_1 = 0.5 \cdot (1 - |S_{11}|^2 - |S_{21}|^2), \tag{7}$$

$$\text{MEG}_2 = 0.5 \cdot (1 - |S_{22}|^2 - |S_{12}|^2). \tag{8}$$

TARC is computed as

$$\text{TARC} = \sqrt{\frac{|S_{11} + S_{12}|^2 + |S_{21} + S_{22}|^2}{2}}. \tag{9}$$

As summarized in Table 2, the proposed dual-band THz antenna exhibits significant advantages over recently published designs in terms of compactness, bandwidth, and radiation performance. With a compact footprint of only $0.40 \times 0.79\,\text{mm}^2$, the antenna achieves dual resonances at 0.372 THz and 0.762 THz, targeting key frequencies in the terahertz band. The corresponding bandwidths of 40 GHz and 60 GHz are notably wider than those of prior works such as [11–14], demonstrating enhanced operational flexibility for broadband THz applications.

In terms of radiation performance, the antenna delivers peak gains of 5.00 dBi and 13.30 dBi at the respective resonant frequencies, surpassing the gain levels of most existing THz antennas, which generally remain below 10 dBi. Furthermore, the antenna maintains a very low Envelope Correlation Coefficient (ECC) below 0.02 across both bands, indicating excellent spatial diversity and minimal mutual coupling – an essential characteristic for high-performance MIMO systems. The corresponding Diversity Gain (DG) remains close to the theoretical maximum of 10, while the Mean Effective Gain (MEG) values lie within the expected range of 0 to 0.5, ensuring a balanced reception capability across different antenna ports.

Additionally, the Total Active Reflection Coefficient (TARC) remains below 3.5 over the operating bands, confirming strong impedance matching even under simultaneous multiport excitation. The simulated Voltage Standing Wave Ratio (VSWR) is maintained around 1.05–1.06, further verifying excellent input matching. Notably, the radiation efficiency of the antenna reaches up to 94%, indicating minimal losses and high radiative effectiveness at terahertz frequencies.

Overall, these results collectively establish the proposed design as a promising candidate for future 6G and ultra-high-speed wireless communication systems operating in the THz regime. The combination of compact size, high gain, wide bandwidth, and strong MIMO characteristics positions this antenna favourably among contemporary state-of-the-art solutions.

4. Conclusion. A compact high-gain two-port MIMO antenna operating across the 0.1–1 THz band has been proposed and analyzed. The design, based on a multi-stage notched microstrip patch architecture and implemented on a polyimide substrate, demonstrates outstanding performance in terms of impedance matching, bandwidth, gain, and mutual coupling. Dual resonances at 0.372 THz and 0.762 THz achieve respective bandwidths of 20 GHz and 60 GHz, with return losses below −30 dB and VSWR values close to unity. The antenna offers significant directional gains of 5.00 dBi and 13.30 dBi, while maintaining an ECC value below 0.02, confirming its excellent diversity performance.

Given its ultra-compact footprint of $0.4 \times 0.79\,\text{mm}^2$ and strong radiation characteristics, the proposed design is highly suitable for future THz wireless systems,

Table 2

Comparison of reported dual-band THz antennas with the proposed design

Reference	**Size (mm^2)**	**Resonant Freq. (THz)**	**Bandwidth (GHz)**	**Max Gain (dBi)**
[11]	0.50×0.50	0.60, 0.70	50	8.36
[12]	0.59×0.59	0.65, 1.13	110	9.45
[13]	1.00×1.20	0.395, 0.629	24	3.19
[14]	2.70×3.65	0.12, 0.17	6	6.24
This work	0.40×0.79	0.372, 0.762	40, 60	5.00, 13.30

including short-range ultra-high-speed communications, nanoscale sensing, and next-generation 6G applications. Future work will focus on fabrication, experimental validation, and performance benchmarking against state-of-the-art THz MIMO antenna structures.

REFERENCES

[1] Ning B., Z. Tian, W. Mei et al. (2023) Beamforming technologies for ultra-massive MIMO in terahertz communications, IEEE Open J. Comm. Soc., **4**, 614–658.

[2] Bodet D. M., J. M. Jornet (2023) Directional antennas for sub-THz and THz MIMO systems: bridging the gap between theory and implementation, IEEE Open J. Comm. Soc., **4**, 2261–2273.

[3] Alibakhshikenari M., B. S. Virdee, A. A. Althuwayb et al. (2021) Compact and low-profile on-chip antenna using underside electromagnetic coupling mechanism for terahertz front-end transceivers, Electronics, **10**(11), 1264.

[4] Raghunath J., P. Kumar, T. Ali et al. (2023) A quad-port nature-inspired lotus-shaped wideband terahertz antenna for wireless applications, J. Sensor Actuator Networks, **12**5, 69.

[5] Benkhallouk K., A. Bendaoudi, M. Berka et al. (2022) Enhanced radiation characteristics of regular dodecagon split ring resonator (D-SRR)-based microstrip patch antenna employing dielectric superstrate for THz applications, J. Eng. Appl. Sci., **69**(1), 71.

[6] Ahammed B., T. Karim, M. A. Alim (2025) Investigation of graphene functionalized multi-band MIMO antenna with enhanced isolation with high gain for THz applications, Discover Electronics, **2**(1), 11.

[7] Amraoui Y., I. Halkhams, R. El Alami et al. (2024) High gain MIMO antenna with multiband characterization for terahertz applications, Scientific African, **26**, e02380.

[8] Amraoui Y., I. Halkhams, R. El Alami et al. (2025) Terahertz dual-band antenna design with improved performances using FSS-based metasurface concept for wireless applications, Scientific African, **27**, e02566, `https://doi.org/10.1016/j.sciaf.2025.e02566`.

[9] Amraoui Y., I. Halkhams, R. El Alami et al. (2024) High isolation MIMO antenna array for multiband terahertz applications, Results Eng., **23**, 102842.

[10] Diez-Comas A., D. M. Bodet, J. M. Jornet (2025) Enabling sub-terahertz broadband MIMO communications with leaky-wave antenna arrays, IEEE Open J. Comm. Soc., **6**, 2293–2307, `https://doi.org/10.1109/OJCOMS.2025.3550308`.

[11] Amraoui Y., I. Halkhams, R. El Alami et al. (2025) Terahertz dual-band antenna design with improved performances using FSS-based metasurface concept for wireless applications, Scientific African, **2025**, e02566, Elsevier.

[12] Halkhams I., R. El Alami, M. O. Jamil et al. (2024) A new approach to designing a multiband antenna using photonic crystals and load graphene for terahertz application, Results in Engineering, **22**, 102327.

[13] Al Ka'bi A., A. Mustafa (2024) Design of MIMO antenna for wideband THz mobile communications, Telecomm. Radio Eng., **83**, Begel House Inc.

[14] Patel S. K., A. Baz, D. Agravat (2025) Design of machine learning optimized THz MIMO antenna for next-generation wireless communication systems, Ain Shams Eng. J., **16**(6), 103384.

[1]*Laboratory of Electronics, Advanced Signal Processing, and Microwave (LESM), Department of Telecommunications, Saida University, Saida 20000, Algeria*
e-mails: abdelbasset.azzouz@univ-saida.dz, rachid.bouhmidi@univ-saida.dz, mohammed.chetioui@univ-saida.dz

[2]*Center for Telecommunication Research & Innovation (CeTRI), Fakulti Teknologi Dan Kejuruteraan Elektronik Dan Komputer (FTKEK), Universiti Teknikal Malaysia Melaka (UTeM), Jalan Hang Tuah Jaya, 76100, Durian Tunggal, Melaka, Malaysia*
e-mails: zahriladha@utem.edu.my, ahmedjamal@ieee.org